

Article

Study on Urban Expansion and Population Density Changes Based on the Inverse S-Shaped Function

Huiyuan Lu [†], Zhengyong Shang ^{*}, Yanling Ruan [†] and Linlin Jiang

School of Geography Science and Geomatics Engineering, Suzhou University of Science and Technology, Suzhou 215009, China

^{*} Correspondence: shangzy@usts.edu.cn; Tel.: +86-181-181-511-69[†] These authors contributed equally to this work.

Abstract: For decades, the continuous advance of urbanization has led to the continuous expansion of urban land and rapid increase in the total area of cities. The phenomenon of urban land expansion faster than population growth has become widespread. High population density can lead to problems such as traffic congestion and exacerbated air pollution and can hinder sustainable development, affecting the quality of life of urban residents. China is currently in a phase of rapid urbanization, with high urban population density and rapid decline in urban population density. The decrease in urban population density is conducive to promoting sustainable urban development. This study selected 34 cities in China as sample cities and analyzed the spatial expansion and population density changes using land use and population density data from 2000, 2005, 2010, 2015, and 2020 in order to provide reference for controlling population density and promoting sustainable urban development. The conclusions of the study are as follows: In the 34 sample cities, the average urban radius was only 11.61 km in 2000, but reached 17.98 km in 2020, with an annual growth rate of 2.5%. There were significant spatial differences in urban expansion. Beijing and Shanghai, as the most developed cities in China, had urban radii exceeding 40 km, while the less developed cities of Liaoyang and Suzhou had urban radii of only 9 km. Although the population density decreased in most cities, the population density values in first-tier cities in China, such as Tianjin, Beijing, and Shanghai, continued to rise. Cities with loose spatial expansion patterns had faster decreases in population density than compact-type cities. The rate of urban spatial expansion was negatively correlated with changes in population density, with cities that had faster urban spatial expansion also having faster declines in artificial ground density.

Keywords: urban spatial expansion; population density; China; urban spatial expansion form



Citation: Lu, H.; Shang, Z.; Ruan, Y.; Jiang, L. Study on Urban Expansion and Population Density Changes Based on the Inverse S-Shaped Function. *Sustainability* **2023**, *15*, 10464. <https://doi.org/10.3390/su151310464>

Academic Editor: Miguel Amado

Received: 24 May 2023

Revised: 21 June 2023

Accepted: 26 June 2023

Published: 3 July 2023



Copyright: © 2023 by the authors. Licensee MDPI, Basel, Switzerland. This article is an open access article distributed under the terms and conditions of the Creative Commons Attribution (CC BY) license (<https://creativecommons.org/licenses/by/4.0/>).

1. Introduction

Cities are the center of economic activities and cultural exchanges, representing the economic and cultural conditions of a region [1]. Therefore, urbanization is an extremely important indicator when evaluating the level of development in a region [2]. Urbanization is mainly manifested by the increase in the proportion of urban population to the total population and the expansion of urban land area [3,4]. At the same time, it also involves a series of processes such as industrial structure upgrading and natural environment development [5–7]. Currently, the measurement of urbanization level in a region mainly includes two indicators: land urbanization and population urbanization [8,9]. Urban development requires a large amount of land and population [10]. In the past few decades, urban land has expanded rapidly around the world, and the total area of cities has multiplied [10,11]. Currently, more than half of the world's population lives in urban areas, and this number is expected to increase to 5 billion by 2030 [12].

During urban expansion, a large amount of cultivated land, forest land, and shrubland is converted to urban land use [13], which leads to many environmental problems such

as urban heat islands [14], increased carbon emissions [15], and urban waterlogging [16], which pose a serious threat to local sustainable development [17,18]. Many scholars have studied the types and spatial forms of urban expansion, as well as the driving forces of urban expansion, in order to provide references for sustainable urban development [19]. The LEI (Landscape Expansion Index) is an index based on the spatiotemporal dynamics of urban land growth. The LEI divides urban expansion types into three categories based on the spatial relationship between newly added urban land and existing urban land: the infilling type, the edge-expansion type, and the outlying type [20]. The LEI can not only quantify the landscape patterns of urban construction land growth but also analyze the process of landscape pattern changes between multiple time points from the perspective of urban landscape research [21]. Jiao proposed an inverse S-shaped urban land density function, which is a function describing the attenuation of urban construction land density with distance. This function can quantify the spatial form of urban expansion [22]. GeoDetector is a commonly used statistical plugin that can be used to detect spatial heterogeneity of geographic factors and reveal their driving forces [23]. Due to its ability to reflect the interaction between driving factors and response variables, GeoDetector has been widely applied in fields such as urban development and ecological security [24–26]. Liu et al. and Xu et al. used the geographic detector to analyze the driving factors of urban spatial expansion and proposed that population is a key factor affecting urban expansion [21,27].

As the cost of childbirth rises and attitudes toward childbirth change, China's birth rate has sharply declined [28]. From a national perspective, in 2022, China's total population experienced negative growth for the first time, indicating that China's population problem has further intensified. Currently, China faces a series of demographic problems such as gender imbalance [29,30], uneven distribution of population [31,32], aging population [33], and decreasing working-age population [34,35]. In the past few decades, due to factors such as abundant labor [36] and resources [37], convenient transportation [38,39], etc., multinational companies have deployed a large number of labor-intensive and resource-oriented industries in China's coastal regions. However, with the increase in China's labor costs and the decrease in the working-age population, the demographic dividend has gradually disappeared, and manufacturing has begun to shift to Southeast Asia, affecting China's economic development [40].

In addition to the impact on economic development, the accelerated process of population aging and the decline in the working-age population will increase social burdens [41,42]. Moreover, the growing number of elderly people due to aging has given rise to a huge service market. However, due to low entry barriers, inadequate punishment, regulation, and management measures in this industry, the quality of service personnel varies greatly, and there are often instances of elder abuse [33,43,44]. To tackle the aging population problem, the government should increase corresponding investment and establish an effective and strict set of industry regulations [33,43]. To address the shortage of working-age population, the promotion of automation and intelligent technology and the development of high-tech industries are urgent. At the urban level, with the improvement in transportation infrastructure, the resistance for rural working-age population to move to cities for employment decreases [45]. A large rural working-age population actively migrate to cities for higher pay and better social welfare [46]. Therefore, urban population growth is rapid, urban demand for land increases, and urban spatial expansion is fast [47]. With the decrease in rural population migration and birth rates, the urban population growth rate slows down, and the rate of urban spatial expansion gradually decreases. Currently, in many parts of China, young people go out to work while the elderly and children stay in rural areas, resulting in a phenomenon of rural hollowness [48]. Some cities are also likely to face a shortage of population. To cope with this change, urban planners and managers should plan urban land reasonably, improve land use efficiency, promote high-quality urban development, and formulate plans and policies that are conducive to sustainable urban development.

The expansion of urban land area is the main indicator of urban spatial expansion [49]. There are three main categories of assessment methods for urban expansion: the first is the boundary assessment method, which defines the “city” based on administrative division data. This method can evaluate urban expansion over a long period but cannot distinguish between urban and rural areas within the “city” [50]. The second is the threshold method, which uses nighttime light data to build a threshold segmentation model, dividing urban and rural areas in remote sensing images, evaluating the urban extent, and calculating the expansion intensity. This method can distinguish between urban and rural areas within the “city” but has limitations in data availability for conducting long-term urban expansion assessments and low segmentation accuracy [51]. The third is the function equation method, which is based on land use data, establishes a function model, defines the urban boundary, and analyzes urban spatial form. Compared to the other two methods, this approach is relatively accurate and suitable for long-term urban expansion assessments. Xuecao Li et al. used global impervious surface data to build a global urban boundary dataset, employing kernel density analysis and domain expansion algorithm [52]. Jianxin Yang et al. explored the process of urban expansion and analyzed urban spatial form based on land use data and Gaussian function model [53]. Jiao Limin constructed the urban land density function based on land use data for 1900, 2000, and 2010 to define the urban scope [22].

In the past few decades, China’s economic growth has provided strong support for urbanization [54–56]. The process of land urbanization and population urbanization in China is rapidly advancing [57–59]. To reveal the relationship between urban expansion and population density changes in the development process of China, this paper selected 34 cities from over 300 cities in China. Based on land use data from 2000 to 2020, the spatial and temporal differences of urban expansion were analyzed using inverse s-shaped function model and Pearson correlation coefficient. On this basis, the correlation between urban expansion and population density changes was explored, providing a reference for sustainable urban development in China.

2. Materials and Methods

2.1. Study Area

China is located in the eastern part of Asia, on the west coast of the Pacific Ocean. Its land area is approximately 9.6 million km², ranking third in the world in terms of land area. China’s GDP grew rapidly following the Reform and Opening Up policy, which promoted the process of urbanization [60,61]. However, due to regional development disparities, significant spatial differences have arisen in both urban expansion and population growth in China [61]. According to data released by the National Bureau of Statistics of China in 2022, China experienced negative population growth for the first time, which has significant implications for the country’s urban development. This study selected 34 cities in China as the study object to analyze the relationship between urban spatial expansion and changes in population density. The research area is shown in Figure 1.

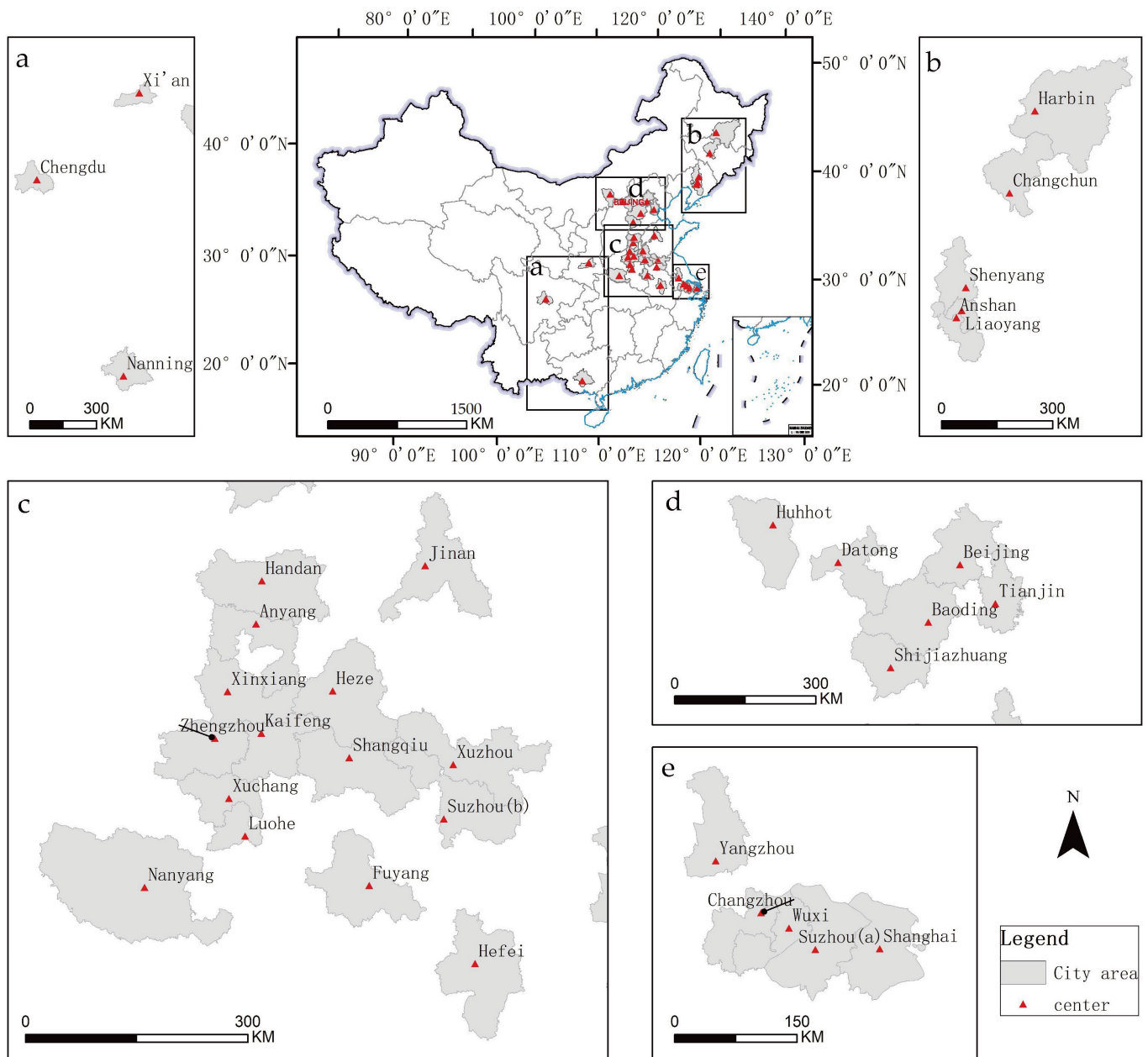


Figure 1. Location of the study area. (a): Xi'an, Chengdu and Nanning. (b): Anshan, Changchun, Harbin, Liaoyang and Shenyang. (c): Anyang, Fuyang, Handan, Hefei, Heze, Jinan, Kaifeng, Luohe, Nanyang, Shangqiu and Suzhou (b), Xinxiang, Xuchang, Xuzhou and Zhengzhou. (d): Beijing, Baoding, Datong, Huhhot, Shijiazhuang and Tianjin. (e): Changzhou, Wuxi, Suzhou (a), Shanghai and Yangzhou.

2.2. Data Sources

This study used land cover data, population data, and administrative division data. The land use and land cover data used in this study were sourced from the CLCD (China Land Cover Dataset) published by Xin Huang and Jie Wang, which was produced using Google Earth Engine and Landsat data. The spatial resolution of CLCD is 30 m, and the overall accuracy is up to 79% [3].

The population density data used in this study were sourced from the WorldPop Project (<https://www.worldpop.org> (accessed on 2 May 2022)), which provides population data from 2000 to 2020 worldwide. The dataset includes two spatial resolutions: 1 km and 100 m [58,59].

The administrative division data used in this study was sourced from the National Fundamental Geographic Information System and National Platform for Common Geospatial Information Services. Please refer to Table 1 for detailed information.

Table 1. Data sources.

Data Name	Data Sources	Resolution
China Land Cover Dataset [3]	zenodo.org (accessed on 2 May 2022)	30 m
population density data	www.worldpop.org (accessed on 2 May 2022)	100 m
administrative division	National Fundamental Geographic Information System National Platform for Common Geospatial Information Services	-

2.3. Methods

The population density of each city can be calculated by obtaining population density data.

$$i_{pop} = \frac{\sum pop_i * area_i}{area} \quad (1)$$

where i_{pop} represents the population density of a city, pop_i represents the population density value corresponding to the i region, $area_i$ represents the area corresponding to the i region, and $area$ refers to the total area of the city.

This study explored the relationship between the density of artificial land surface and distance using multiple ring buffers and an inverse S-shaped function model. This study explored the relationship between the density of impervious surfaces and distance using multiple ring buffers and inverse S-shaped function model. Based on the land cover data from China's Land Cover Dataset in 2000, 2005, 2010, 2015, and 2020, the impervious surface density was calculated for each layer by taking the city center as the starting point and buffering outward every 1 km. The city center was selected based on the CLCD data and verified using satellite imagery provided by Baidu Map [62]. The formula for calculating urban land density is as follows:

$$Den = \frac{S_{bu}}{S_{rin} - S_{wa}} \quad (2)$$

where Den is the urban land density, S_{bu} represents the artificial surface area within the buffer zone, S_{rin} is the area of the buffer zone, and S_{wa} is the water area within the buffer zone.

$$Den = \frac{1 - c}{1 + e^{a((\frac{2r}{d}) - 1)}} + c \quad (3)$$

where Den is the urban land density, e is Euler's number, c is the land density at the edges of a city, r is the distance to the city center, " a " is the parameter that controls the slope of the function, and d is the city radius. The equation is shown in Figure 2.

$$Kp = \frac{r_0}{d} = \frac{1.316957}{a} \quad (4)$$

where Kp refers to urban spatial compactness, which is determined by the ratio between the range of rapid decrease in artificial surface density and the radius of the city. It can be calculated using the parameter " a ". If the value of Kp decreases over time, it indicates that the spatial form of the city is developing toward a more compact type. r_0 is the radius of the inner city area, and d is the radius of the entire city.

The formula for calculating the rate of urban spatial expansion based on the fitted city radius value d is as follows:

$$v = \sqrt[n]{\frac{Dt}{D0}} - 1 \quad (5)$$

Formula (5) is used in this study to calculate the rates of urban spatial expansion and population density growth. The formula uses the value of the element at time point Dt , the value at the previous time point $D0$, and n represents the length of the study period in years.

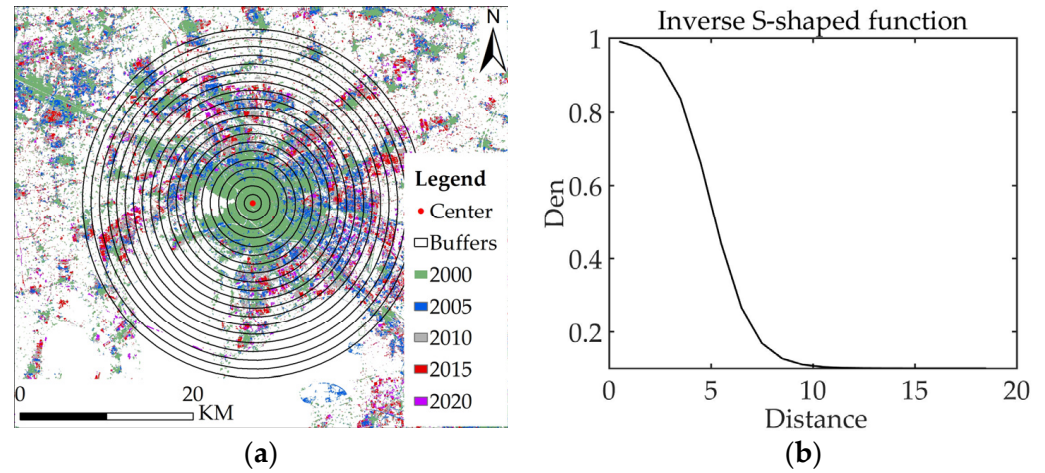


Figure 2. Extracting and shaping urban land density function (a). A schematic diagram of extracting urban land density function using multi-ring buffer (b). Fitting urban land density function, at $a = 5$, $c = 0$, and $d = 10$.

3. Results

3.1. Land Use Change

According to the land use data during the study period, an analysis of the dynamic changes in land use and land cover is presented in Tables 2–4. For detailed parameters, please refer to Table A1 (Appendix A).

Table 2. Land use transfer matrix from 2000 to 2020 (km²).

	Cropland	Forest	Shrub	Grassland	Water	Snow	Barren	Impervious	Wetland
Cropland	-	4181.64	6.40	3559.71	1202.66	0.00	25.00	137.74	14.26
Forest	4501.14	-	231.00	2229.17	19.04	0.00	0.11	0.71	2.13
Shrub	1.84	140.86	-	189.55	0.00	0.00	0.00	0.00	0.00
Grassland	3017.66	113.57	146.26	-	3.88	0.02	44.02	0.47	0.02
Water	2060.38	21.78	0.00	29.56	-	0.00	10.98	423.71	0.62
Snow	0.00	0.00	0.00	0.02	0.02	-	0.04	1.79	0.00
Barren	9.28	0.32	0.07	20.61	5.53	0.00	-	0.00	0.00
Impervious	21,538.71	195.71	0.29	491.23	625.08	0.00	33.82	-	0.05
Wetland	0.24	0.00	0.00	0.12	0.11	0.00	0.00	0.01	-

Table 3. Land use type area from 2000 to 2020 (km²).

	Cropland	Forest	Shrub	Grassland	Water	Snow	Barren	Impervious	Wetland
2000	256,855.25	70,145.09	621.90	25,550.79	9220.58	0.04	126.14	37,704.95	28.91
2005	251,159.99	70,251.21	722.90	25,153.69	10,103.05	0.03	93.56	42,748.08	21.12
2010	244,594.54	70,657.32	544.70	25,134.54	10,250.76	0.06	82.10	48,972.03	17.57
2015	237,671.34	71,523.43	638.57	24,106.23	10,247.96	0.03	62.05	55,990.90	13.12
2020	234,853.40	72,474.50	570.13	22,356.72	9911.28	0.10	49.78	60,025.41	12.30

Table 4. Land use type proportion from 2000 to 2020 (%).

	Cropland	Forest	Shrub	Grassland	Water	Snow	Barren	Impervious	Wetland
2000	64.17	17.53	0.16	6.38	2.30	0.00	0.03	9.42	0.01
2005	62.75	17.55	0.18	6.28	2.52	0.00	0.02	10.68	0.01
2010	61.11	17.65	0.14	6.28	2.56	0.00	0.02	12.24	0.00
2015	59.38	17.87	0.16	6.02	2.56	0.00	0.02	13.99	0.00
2020	58.68	18.11	0.14	5.59	2.48	0.00	0.01	15.00	0.00

According to the land use transfer matrix (Table 2), land use type area (Table 3) and land use type proportion (Table 4), the land use changes from 2000 to 2020 were analyzed. The areas of impervious land and cropland had the highest changes, with an increase of 22,320.46 km² for impervious land and a decrease of 22,001.84 km² for cropland. The increase in impervious land area was mainly due to the conversion from cropland. Cropland decreased by 22,001.84 km², resulting in a decrease in its proportion from 64.2% to 58.7%. Forest increased by 2329.42 km², with its proportion rising from 17.53% to 18.11%. The proportion of impervious land increased from 9.42% to 15.00%, with an increase of 22,320.46 km². Grassland decreased by 3194.07 km², resulting in a decrease in its proportion from 6.38% to 5.59%. Wetland increased by 690.70 km², with its proportion rising from 2.30% to 2.48%. Shrub, snow, barren, and wetland had relatively small areas and insignificant changes.

3.2. Changes in Population Density

Population density data was extracted from the WorldPOP dataset to analyze changes in urban population density. The detailed data are shown in Table 5.

In 2000, the average urban population density of sample cities was 3355 people/km². Heze had the smallest population density in 2032 people/km², and Nanning had the highest population density of 7353 people/km². In 2005, the average urban population density of sample cities was 2913 people/km². Heze had the smallest population density of 1695 people/km², and Nanning had the highest population density of 6010 people/km². In 2010, the average urban population density of sample cities was 2461 people/km². Heze had the smallest population density of 1429 people/km², and Nanning had the highest population density of 4662 people/km². In 2015, the average urban population density of sample cities was 2229 people/km². Heze had the smallest population density of 1234 people/km², and Chengdu had the highest population density of 4377 people/km². In 2020, the average urban population density of sample cities was 2202 people/km². Heze had the smallest population density of 1113 people/km², and Shanghai had the highest population density of 4893 people/km².

The mean rate of change in urban population density between 2000 and 2005 was -0.026 . Xi'an had the fastest decrease in population density, while Datong had the slowest. The mean rate of change in urban population density between 2005 and 2010 was -0.032 . Only Beijing experienced positive growth in urban population density. Hefei had the fastest decrease in population density, while Beijing had the slowest. The mean rate of change in urban population density between 2010 and 2015 was -0.022 . Six cities, including Changzhou, Wuxi, Beijing, Chengdu, Tianjin, and Shanghai, experienced positive growth in urban population density. Suzhou(a) had the fastest decrease in population density, while Shanghai had the slowest. The mean rate of change in urban population density between 2015 and 2020 was -0.006 . Several cities, including Harbin, Zhengzhou, Xi'an, Huhhot, Jinan, Suzhou(a), Wuxi, Changzhou, Tianjin, Beijing, Chengdu, and Shanghai, experienced positive growth in population density. Fuyang had the fastest decrease in population density, while Beijing had the slowest.

Table 5. Sample city population density (people/km²) and population density change rate.

City	Time									
	2000	2005	2010	2015	2020	2000–2005	2005–2010	2010–2015	2015–2020	2000–2020
Anshan	3542	3077	2260	2041	2015	−0.0278	−0.0598	−0.0202	−0.0025	−0.0278
Anyang	3378	2810	2177	1782	1514	−0.0362	−0.0497	−0.0392	−0.0321	−0.0393
Baoding	2917	2467	2162	1830	1751	−0.0330	−0.0261	−0.0328	−0.0088	−0.0252
Beijing	2426	2257	2283	2391	2754	−0.0143	0.0022	0.0093	0.0287	0.0064
Changchun	2595	2215	1804	1486	1357	−0.0312	−0.0402	−0.0380	−0.0180	−0.0319
Changzhou	3540	2856	2338	2358	2525	−0.0421	−0.0392	0.0017	0.0138	−0.0167
Chengdu	5275	4466	4242	4377	4744	−0.0327	−0.0103	0.0063	0.0162	−0.0053
Datong	2600	2557	2388	2187	2152	−0.0034	−0.0136	−0.0174	−0.0032	−0.0094
Fuyang	4066	3417	2320	1726	1375	−0.0342	−0.0745	−0.0574	−0.0445	−0.0528
Handan	2337	2113	1921	1767	1742	−0.0199	−0.0189	−0.0165	−0.0029	−0.0146
Harbin	3498	3406	3144	2851	2853	−0.0054	−0.0158	−0.0194	0.0002	−0.0101
Hefei	5370	4184	2765	2377	2054	−0.0487	−0.0795	−0.0298	−0.0288	−0.0469
Heze	2032	1695	1429	1234	1113	−0.0356	−0.0335	−0.0289	−0.0204	−0.0296
Huhot	3097	2792	2152	1851	1869	−0.0206	−0.0508	−0.0297	0.0020	−0.0249
Jinan	2619	2489	2361	2307	2362	−0.0102	−0.0105	−0.0046	0.0047	−0.0052
Kaifeng	2247	2017	1884	1729	1608	−0.0213	−0.0135	−0.0171	−0.0144	−0.0166
Liaoyang	2327	2187	2043	1884	1856	−0.0123	−0.0136	−0.0160	−0.0030	−0.0112
Luohe	3044	2696	2288	1968	1808	−0.0240	−0.0323	−0.0296	−0.0168	−0.0257
Nanning	7323	6010	4662	3813	3467	−0.0388	−0.0495	−0.0394	−0.0188	−0.0367
Nanyang	2482	2326	2087	1855	1790	−0.0129	−0.0215	−0.0233	−0.0072	−0.0162
Shanghai	4234	4020	3951	4320	4893	−0.0103	−0.0034	0.0180	0.0252	0.0073
Shangqiu	2089	1812	1556	1335	1161	−0.0281	−0.0300	−0.0302	−0.0276	−0.0290
Shenyang	2608	2362	2141	1808	1789	−0.0197	−0.0194	−0.0333	−0.0021	−0.0187
Shijiazhuang	2881	2787	2546	2179	2156	−0.0066	−0.0179	−0.0306	−0.0021	−0.0144
Suzhou (a)	4221	3349	2912	2882	3034	−0.0452	−0.0276	−0.0021	0.0104	−0.0164
Suzhou (b)	4379	3668	2521	1751	1605	−0.0348	−0.0723	−0.0703	−0.0173	−0.0490
Tianjin	2815	2705	2633	2788	3108	−0.0079	−0.0054	0.0115	0.0220	0.0050
Wuxi	3634	3182	2747	2811	2978	−0.0262	−0.0289	0.0046	0.0116	−0.0099
Xi'an	4276	3159	2604	2349	2365	−0.0587	−0.0379	−0.0204	0.0014	−0.0292
Xinxiang	2894	2666	2411	2249	2114	−0.0163	−0.0199	−0.0138	−0.0123	−0.0156
Xuchang	3488	3088	2477	1976	1792	−0.0241	−0.0432	−0.0441	−0.0194	−0.0328
Xuzhou	3773	2894	1944	1520	1318	−0.0517	−0.0765	−0.0480	−0.0282	−0.0512
Yangzhou	3190	2779	2341	1983	1827	−0.0272	−0.0337	−0.0327	−0.0162	−0.0275
Zhengzhou	2863	2535	2191	2012	2016	−0.0240	−0.0287	−0.0169	0.0003	−0.0174

3.3. Urban Spatial Expansion and Changes in Population Density

Based on the inverse S-shaped function, the urban land density function of the sample city is calculated. The mean R^2 value of the function is 0.99, with a minimum value of 0.95, indicating high fitting accuracy and accurate reflection of changes in urban land density.

The inverse S-shaped function (urban land density function) is shown in Figures 3 and 4 and Table 6. For detailed parameters, please refer to Table A1 (Appendix A).

- (1) The parameter “a” is the slope parameter of the function, which reflects the compactness of urban space. The higher the value of parameter “a”, the higher the ratio of land density between the core area and suburban area, and the more compact the urban space. In the sample city, the range of parameter “a” is 2.63–6.00. During the study period, the average value of parameter “a” in the sample city decreased year by year, with values of 4.43 (2000), 4.25 (2005), 4.15 (2010), 4.03 (2015), and 4.00 (2020), indicating a transformation from compact to loose urban spatial form.
- (2) Parameter “c” represents the land density value of the urban fringe area, with a range of 0.02–0.44 in the sample city. Cities such as Tianjin, Beijing, and Liaoyang have high land density values in their urban fringe areas due to urban expansion leading to urban integration.

- (3) Parameter “d” represents the radius of the city. In the sample cities, it includes large cities with radii exceeding 40 km, such as Beijing and Shanghai, as well as small cities with radii less than 10 km. The range of city radius in the sample cities is between 5.00 and 44.28 km. The average value of city radius has been increasing year by year, with values of 11.61 (2000), 13.29 (2005), 15.35 (2010), 17.01 (2015), and 17.95 (2020).

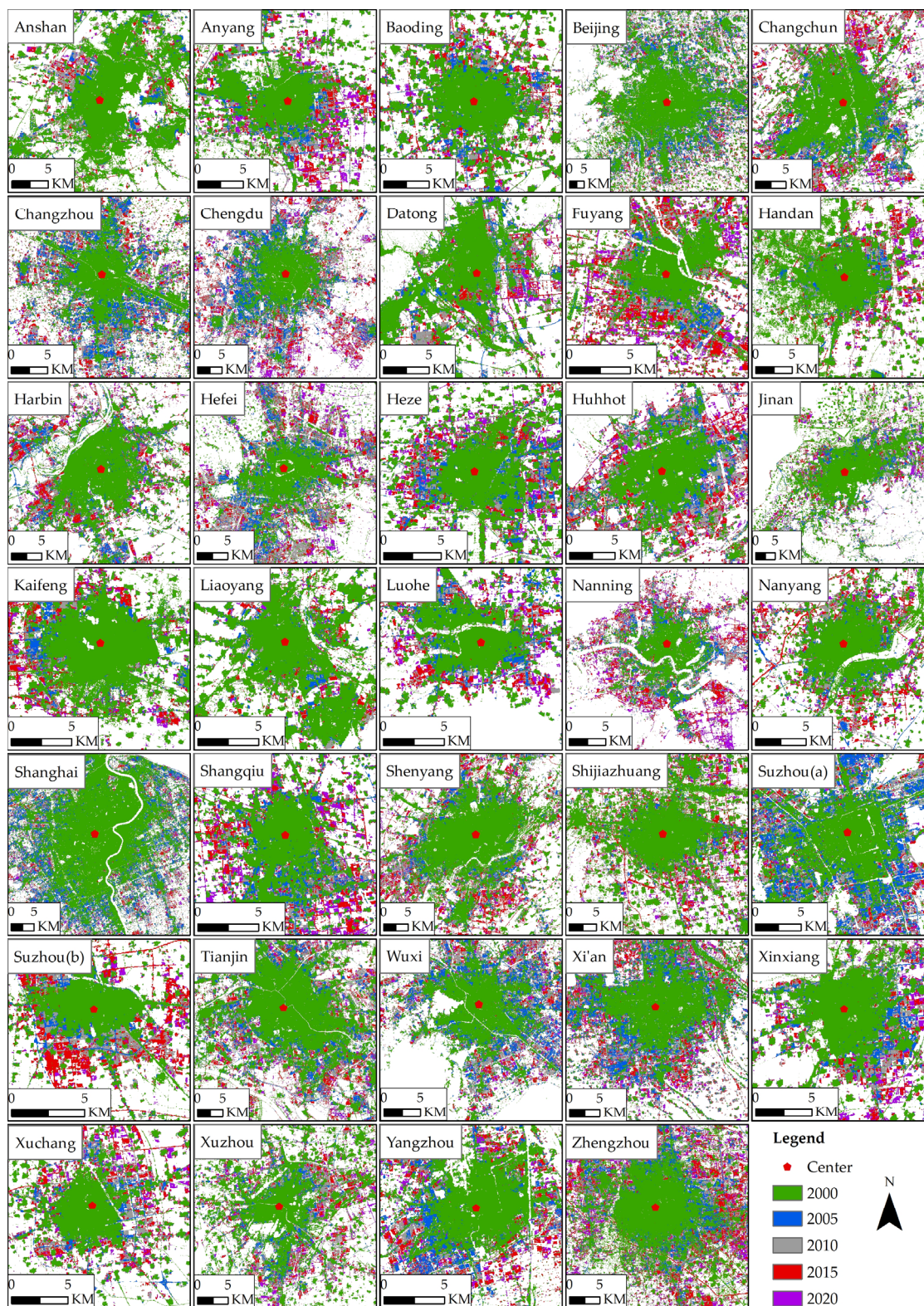


Figure 3. Urban expansion of sample cities.

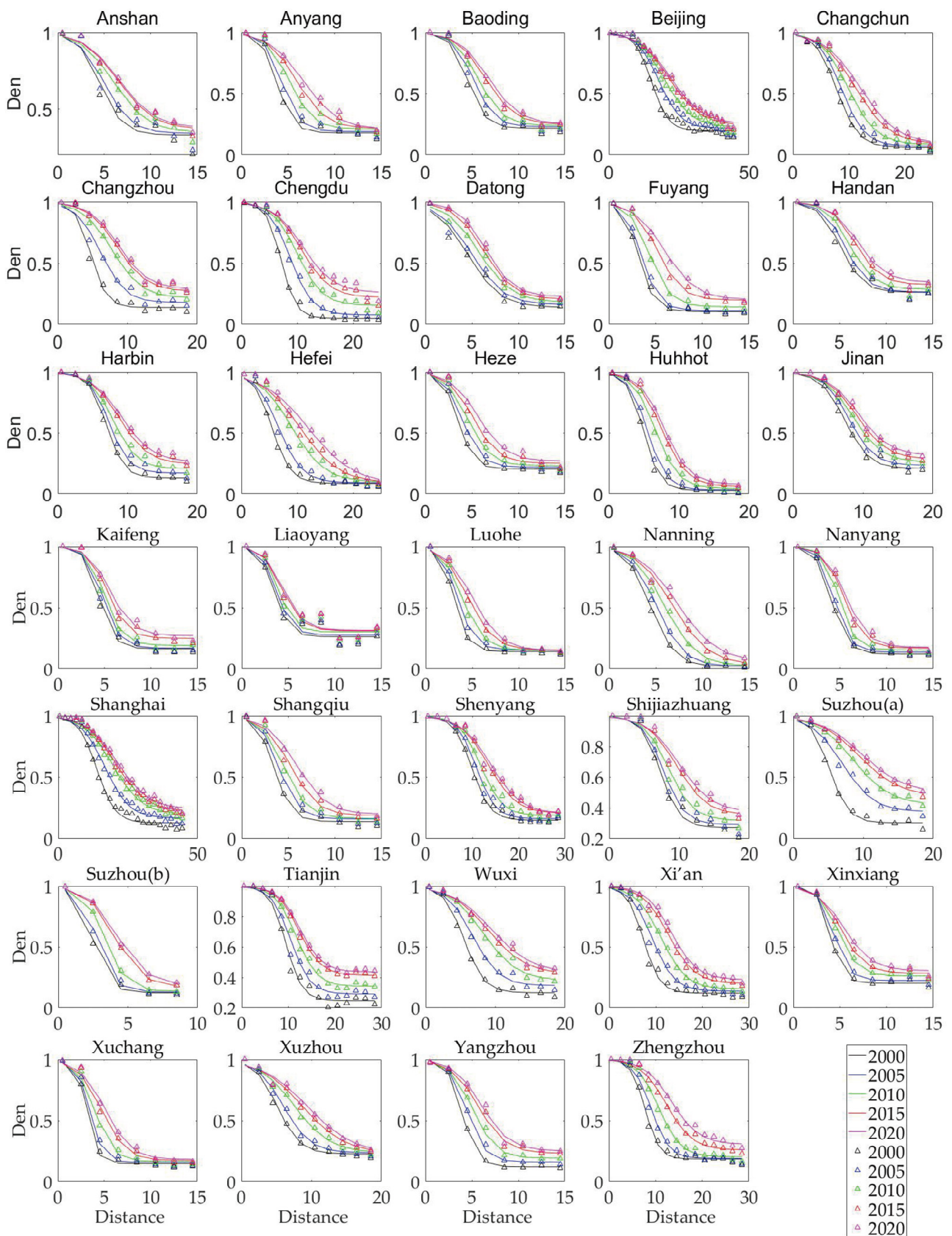


Figure 4. The urban land density (points) and inverse s-shaped function (line) of 34 sample cities.

Table 6. Parameters of the inverse S-shaped function.

Year		2000	2005	2010	2015	2020
a	Minimum	2.632	2.809	2.983	2.874	2.868
	Maximum	5.998	5.342	5.779	5.253	5.341
	Mean	4.431	4.245	4.151	4.029	4.005
	Standard deviation	0.765	0.712	0.668	0.570	0.556
c	Minimum	0.021	0.023	0.025	0.035	0.061
	Maximum	0.328	0.339	0.345	0.414	0.437
	Mean	0.157	0.177	0.200	0.229	0.243
	Standard deviation	0.071	0.072	0.076	0.085	0.089
d	Minimum	4.998	5.538	6.698	8.140	8.515
	Maximum	30.490	35.640	39.820	43.230	44.280
	Mean	11.611	13.294	15.348	17.042	17.980
	Standard deviation	5.798	6.885	7.815	8.353	8.541
r	Minimum	0.950	0.955	0.962	0.963	0.964
	Maximum	0.999	0.998	0.998	0.999	0.998
	Mean	0.989	0.989	0.990	0.990	0.989
	Standard deviation	0.010	0.009	0.006	0.006	0.006

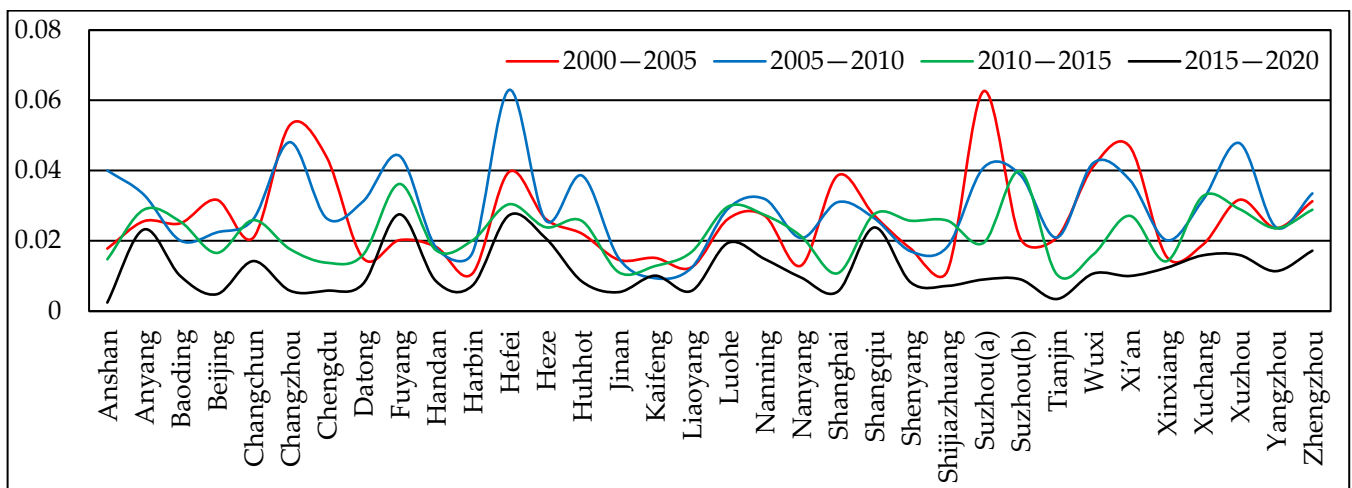
Between 2000 and 2005, the average urban spatial expansion rate was 0.026, with Harbin having the smallest rate at 0.011 and Suzhou(a) having the largest rate at 0.063. There was a strong negative correlation between the urban spatial expansion rate and population density change rate, with a Pearson correlation coefficient of -0.655 . Between 2005 and 2010, the average urban spatial expansion rate was 0.029, with Kaifeng having the smallest rate at 0.009 and Hefei having the largest rate at 0.063. There was a strong negative correlation between the urban spatial expansion rate and population density change rate, with a Pearson correlation coefficient of -0.760 . Between 2010 and 2015, the average urban spatial expansion rate was 0.022, with Tianjin having the smallest rate at 0.010 and Suzhou(b) having the largest rate at 0.040. There was a very strong negative correlation between the urban spatial expansion rate and population density change rate, with a Pearson correlation coefficient of -0.868 . Between 2015 and 2020, the average urban spatial expansion rate was 0.012, with Anshan having the smallest rate at 0.002 and Fuyang having the largest rate at 0.028. There was a strong negative correlation between the urban spatial expansion rate and population density change rate, with a Pearson correlation coefficient of -0.813 .

3.4. Urban Spatial Expansion Form and Changes in Population Density

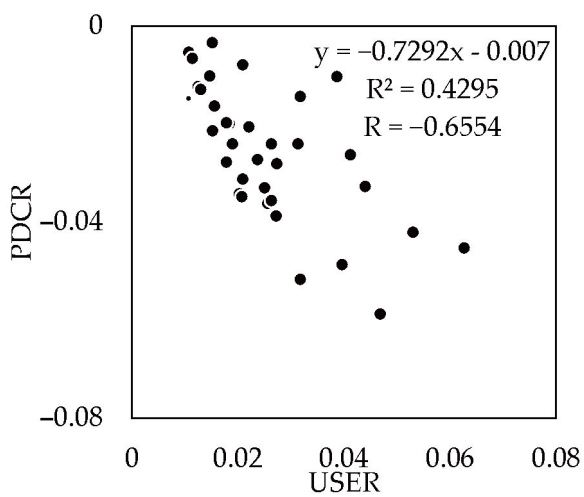
Calculation urban spatial compactness K_p , where K_p represents the ratio of the range of decrease in urban land density to the city radius and can be used to analyze urban spatial growth patterns. If the increase in K_p value exceeds 0.01 compared to the previous time point, the urban spatial growth pattern is the loose type; if the decrease in K_p value exceeds 0.01, the urban spatial growth pattern is the compact type; if the change in K_p value is less than 0.1, it is considered the stable type. The correlation between urban space expansion and population density changes is shown in Figure 5, while the relationship between urban spatial expansion patterns and population density changes is illustrated in Figure 6.

Between 2000 and 2020, the average K_p values of 34 sample cities were 0.3069 (2000), 0.3195 (2005), 0.3254 (2010), 0.3334 (2015), and 0.3353 (2020). Only five cities, Datong, Xi'an, Handan, Huhhot, and Nanning, had decreasing K_p values.

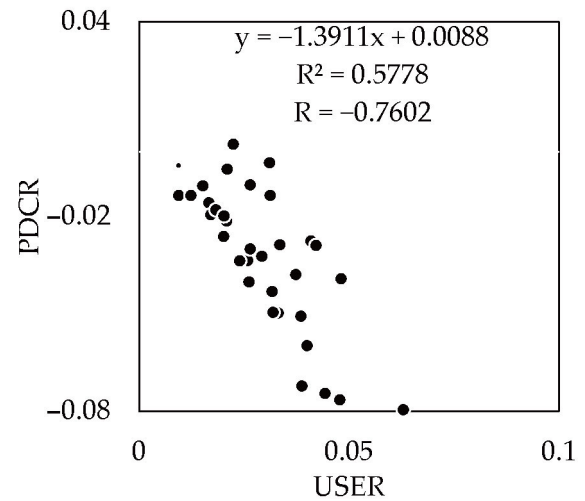
Specifically, from 2000 to 2005, the average K_p value of sample cities increased by 0.0128. Datong had the largest decrease in K_p value, reaching 0.0315, while Suzhou had the largest increase, at 0.0748. The number of loose type, stable type, and compact type cities were 19, 9, and 6, respectively.



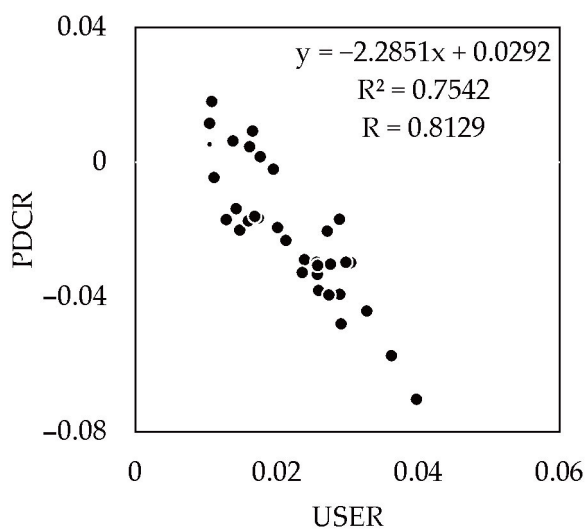
(a) Urban spatial expansion rates



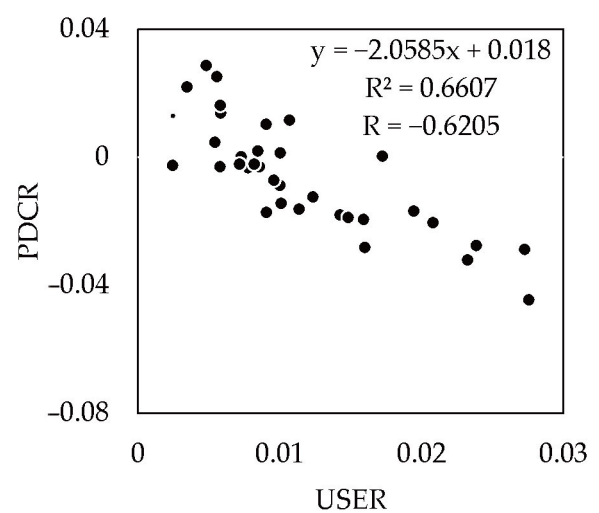
(b) 2000–2005



(c) 2005–2010



(d) 2010–2015



(e) 2015–2020

Figure 5. Urban spatial expansion and changes in population density and their correlation. (a) Urban spatial expansion rates (USER). (b–e) The correlation between urban spatial expansion rates (USER) and population density change rates (PDCR) from 2000 to 2020.

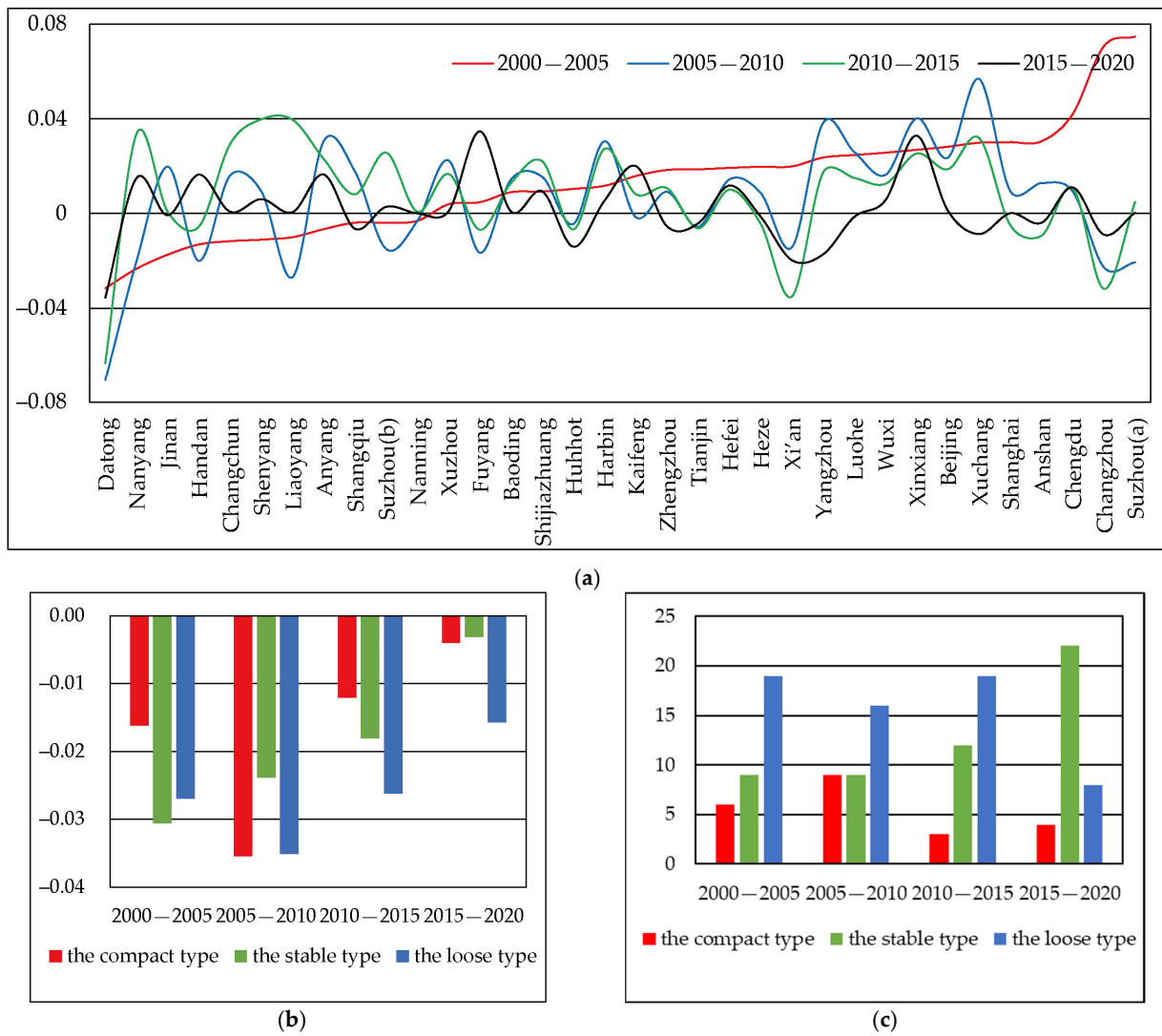


Figure 6. The relationship between urban spatial expansion forms and population density changes. (a) Changes in the KP value of sample cities from 2000 to 2020. (b) Population density change rates of three types of urban spatial expansion forms. (c) The quantity of three types of urban spatial expansion forms.

From 2005 to 2010, the average Kp value of sample cities increased by 0.0059. Datong had the largest decrease in Kp value, reaching 0.0707, while Xuchang had the largest increase, at 0.0569. The number of loose type, stable type, and compact type cities were 16, 9, and 9, respectively.

From 2010 to 2015, the average Kp value of sample cities increased by 0.0059. Datong had the largest decrease in Kp value, reaching 0.0633, while Shenyang had the largest increase, at 0.0399. The number of loose type, stable type, and compact type cities were 19, 12, and 3, respectively.

From 2015 to 2020, the average Kp value of sample cities increased by 0.0019. Datong had the largest decrease in Kp value, reaching 0.0355, while Fuyang had the largest increase, at 0.0347. The number of loose type, stable type, and compact type cities were 8, 22, and 4, respectively.

Before 2015, loose-type cities dominated urban spatial expansion, while after 2015, stable-type cities became the dominant form. The number of stable-type cities increased from 9 to 22. The average Kp value change rate of the sample cities decreased year by year. Except for 2005–2010, the population density decline rate of compact-type cities was slightly faster than that of loose-type cities. In other periods, when the urban spatial

expansion form was loose type, the population density decline rate was faster than that of compact-type cities.

4. Discussion

During the early stage of urbanization in China, while transportation facilities gradually improved, there existed significant discrepancies in economic and social security levels among different cities. To obtain better salaries and benefits, workers actively migrated to cities with superior economic conditions, leading to massive population mobility. From 2000 to 2010, the permanent populations of some cities almost doubled [63,64]. The rapid population and economic growth promoted urban spatial expansion. After the 2008 financial crisis, the cost of living in urban areas gradually increased, particularly with the rapid rise of housing prices. The increase in housing prices is closely related to China's household registration, education system, and population size. Due to the high degree of integration between housing, household registration, and education in economically developed urban areas with large populations, housing prices surged, lowering incentives for childbirth and residency within these regions [65].

Population is the most commonly used indicator when examining the driving factors that cause urban expansion [47,66,67]. In 2022, China's population experienced negative growth for the first time, while China's urbanization rate reached 65.22%. This is of immense significance for China's urban development. As the urbanization process advances, the number of rural laborers entering cities to settle will gradually decrease. The concept of utilizing demographic dividends to promote urban sustainable development is gradually losing its feasibility due to this phenomenon. However, a decrease in the total population can promote high-quality urban development. Due to its massive population size, cities consume large amounts of resources, generate a lot of pollutants, and face challenges in environmental governance [68,69]. A reduction in the total population can help alleviate resource and environmental pressures, improve environmental quality, and promote sustainable development [70]. A decrease in the population can also promote the development of high-tech and high value-added industries by enterprises, improving production efficiency and reducing labor costs, as well as pushing forward the development of intelligent and mechanized industries. Given that China's housing prices rapidly increased due to the quick population and economic growth in the past, a decrease in the population can also help "cool down" the real estate market [71–73]. This study explores the relationship between the speed and form of urban spatial expansion and changes in population density, which has positive implications for handling the relationship between space and population growth, promoting sustainable urban development, and achieving high-quality urban development.

5. Conclusions

This study utilized an inverse S-shaped function and remote sensing data to analyze the spatial and temporal differences in urban expansion and population density changes in China, exploring the inherent correlation between urban expansion and population density data, and analyzing the impact of urban spatial form on urban expansion. The conclusions are as follows:

- (1) The impervious surface area is rapidly increasing, which is leading to the occupation of a significant amount of agricultural land. However, due to China's substantial investment in ecological conservation, the forest area has increased by 2329.42 km². There has also been a conversion between four types of land cover: forest, grassland, water, and cropland. (2) Since the implementation of China's Reform and Opening Up policy, there has been rapid development in both the country's economy and society. One of the resulting effects has been the swift expansion of urban impervious land. A study conducted across 34 sample cities reveals that the average radius of urban areas increased from 11.61 km in 2000 to 17.98 km in 2020, representing an annual growth rate of 2.5%. The city radius varies considerably across these

cities, as exemplified by Beijing and Shanghai's city radius of over 40 km, while Liaoyang and Suzhou(b), cities with lower development levels, have a radius of 9 km. Half of the sample cities measured had a radius of 15 km. Alongside the size differences between sample cities, the urban expansion rates also differ noticeably. For instance, Hefei and Suzhou exhibited annual average urban spatial expansion rates of 16.7% and 13.8%, respectively, whereas Jinan and Liaoyang grew at only 4.8% and 4.7% each year. (3) The urban spatial form is predominantly characterized by the loose type, and the average K_p continues to decline. China's urban population density has been consistently decreasing, which has a negative correlation with the expansion rate of urban areas. Cities featuring the loose type of spatial form tend to exhibit a faster decrease in population density compared to other types of cities. (4) The decline in urban population density is not only caused by urban expansion but also by a decrease in population growth rate. This decrease can be attributed to economic development, increased salaries, job opportunities and higher living standards. As regions become more developed, they may become less attractive due to lower salary levels and fewer protections for employees, resulting in a decrease in cross-city commuting populations. Furthermore, the decline in population growth rate can be linked to rising housing and commodity prices, which increase the cost of living and having children in cities. This factor leads people to reconsider their attitudes toward having children and can ultimately impact natural population growth rates. There are notable disparities in the rates of expansion among different cities. Temporally, the primary factor contributing to the variance in urban radii growth rates is due to early stage cities having small radii, abundant undeveloped land, and low construction expenses, which results in faster growth. As cities continue to develop and expand their radii, the availability of unused land decreases while construction costs soar, leading to a significant decline in the rate of urban radius growth. In order to increase revenue and improve resource utilization efficiency, many industries choose to locate in underdeveloped areas. From a spatial perspective, the uneven socioeconomic foundations of each city constitute the main cause for different rates of urban radius expansion. Cities with prosperous economic conditions generally possess robust infrastructure, active commercial activities, and abundant employment opportunities, all of which attract a large number of immigrants and promote rapid urban expansion.

Author Contributions: Conceptualization, Z.S.; methodology, Z.S. and H.L.; software, H.L. and Y.R.; validation, Y.R., H.L. and Z.S.; formal analysis, H.L.; investigation, H.L. and L.J.; resources, L.J. and H.L.; data curation, L.J. and H.L.; writing—original draft preparation, H.L.; writing—review and editing, H.L. and Z.S.; visualization, H.L. and Y.R.; supervision, Z.S.; project administration, Z.S.; funding acquisition, Z.S. and H.L. All authors have read and agreed to the published version of the manuscript.

Funding: This research was funded by the National Natural Science Foundation of China (no. 41371171), Starting Research Program of Suzhou University of Science and Technology (no. 331812116) and University Students Innovation and Entrepreneurship Training Program Fund Project of Jiangsu Province (no. 202210332083Y).

Institutional Review Board Statement: Not applicable.

Informed Consent Statement: Not applicable.

Data Availability Statement: The data presented in this study are available on request from the corresponding author.

Acknowledgments: We thank the Google Earth Engine platform, National Earth System Science Data Center, National Fundamental Geographic Information System, WorldPop Project (www.worldpop.org) (accessed on 2 May 2022) and National Platform for Common Geo-spatial Information Services.

Conflicts of Interest: The authors declare no conflict of interest.

Appendix A

Table A1. Parameters of the inverse S-shape function of the sample cities.

City	2000				2005				2010				2015				2020			
	a	c	d	r	a	c	d	r	a	c	d	r	a	c	d	r	a	c	d	r
Anshan	3.75	0.33	9.11	0.95	3.45	0.34	9.95	0.95	3.34	0.34	12.11	0.98	3.42	0.37	13.03	0.98	3.46	0.38	13.19	0.99
Anyang	4.43	0.18	7.68	0.98	4.53	0.19	8.72	0.99	4.10	0.21	10.26	0.99	3.82	0.21	11.83	0.98	3.65	0.21	13.27	0.99
Baoding	4.80	0.22	9.12	0.99	4.64	0.23	10.32	0.99	4.42	0.24	11.40	0.99	4.24	0.25	12.93	0.99	4.22	0.25	13.59	0.99
Beijing	4.96	0.19	30.49	0.99	4.48	0.21	35.64	0.99	4.15	0.23	39.82	0.99	3.92	0.24	43.23	0.99	3.90	0.25	44.28	0.99
Changchun	4.09	0.06	15.69	1.00	4.24	0.07	17.40	0.99	4.03	0.09	19.80	0.99	3.70	0.09	22.50	0.99	3.69	0.09	24.15	0.99
Changzhou	4.22	0.14	9.48	0.99	3.44	0.18	12.27	0.99	3.66	0.22	15.52	0.99	4.01	0.27	16.94	0.99	4.12	0.29	17.44	0.99
Chengdu	5.32	0.05	14.17	1.00	4.54	0.08	17.57	0.99	4.40	0.15	20.02	0.99	4.25	0.22	21.44	0.98	4.10	0.26	22.07	0.98
Datong	2.63	0.14	9.17	0.98	2.81	0.16	9.88	0.99	3.31	0.18	11.52	0.99	3.93	0.21	12.47	0.99	4.40	0.23	12.96	0.99
Fuyang	3.79	0.10	6.37	0.99	3.74	0.11	7.04	0.99	3.92	0.14	8.74	1.00	4.00	0.20	10.44	0.99	3.62	0.20	11.96	0.99
Handan	4.40	0.26	10.21	0.98	4.60	0.27	11.18	0.99	4.94	0.29	12.23	0.99	5.05	0.32	13.33	0.99	4.75	0.34	13.91	0.99
Harbin	5.47	0.13	13.93	0.99	5.22	0.17	14.69	0.99	4.66	0.20	15.95	0.99	4.24	0.25	17.62	0.99	4.17	0.26	18.27	0.99
Hefei	3.32	0.09	10.96	0.99	3.16	0.09	13.31	0.99	3.06	0.10	18.06	0.99	2.99	0.09	20.98	0.99	2.91	0.08	24.00	0.98
Heze	4.17	0.20	7.04	0.99	3.92	0.22	8.01	0.99	3.82	0.23	9.10	0.99	3.87	0.25	10.24	0.99	3.89	0.27	11.35	0.99
Huhhot	4.24	0.03	9.90	0.99	4.10	0.03	11.04	0.99	4.16	0.05	13.34	1.00	4.25	0.06	15.14	1.00	4.45	0.08	15.79	1.00
Jinan	4.27	0.20	14.86	0.99	4.52	0.23	15.98	0.99	4.23	0.26	17.23	0.99	4.22	0.28	18.21	0.99	4.23	0.31	18.71	0.99
Kaifeng	5.52	0.16	8.87	0.99	5.17	0.17	9.56	0.99	5.21	0.19	10.02	0.99	5.04	0.25	10.68	0.99	4.68	0.27	11.23	0.99
Liaoyang	4.27	0.26	7.02	0.96	4.41	0.28	7.47	0.96	4.84	0.30	7.95	0.96	4.23	0.31	8.64	0.96	4.22	0.32	8.89	0.96
Luohe	4.12	0.14	6.06	0.99	3.82	0.15	6.90	0.99	3.56	0.15	7.97	0.99	3.42	0.15	9.23	0.99	3.43	0.15	10.16	0.99
Nanning	3.53	0.02	8.90	1.00	3.56	0.02	10.17	1.00	3.59	0.02	11.90	0.99	3.58	0.04	13.62	0.99	3.58	0.06	14.66	0.99
Nanyang	4.85	0.12	8.27	1.00	5.31	0.14	8.82	1.00	5.78	0.15	9.77	1.00	5.04	0.17	10.86	0.99	4.76	0.17	11.39	0.99
Shanghai	4.18	0.13	27.81	0.99	3.82	0.16	33.61	0.99	3.71	0.20	39.16	0.99	3.77	0.22	41.32	0.99	3.77	0.24	42.48	0.99
Shangqiu	3.82	0.14	7.02	0.99	3.87	0.16	8.03	0.99	3.68	0.16	9.15	0.99	3.59	0.18	10.48	0.99	3.66	0.20	11.79	0.99
Shenyang	5.06	0.15	19.93	1.00	5.28	0.16	21.77	0.99	5.09	0.18	23.69	0.99	4.41	0.20	26.90	0.99	4.32	0.20	28.02	0.99
Shijiazhuang	5.33	0.27	14.62	0.99	5.14	0.29	15.47	0.98	4.85	0.32	16.94	0.98	4.48	0.35	19.24	0.98	4.34	0.37	19.94	0.98
Suzhou(a)	3.86	0.13	10.37	0.99	3.16	0.22	14.05	0.99	3.33	0.28	17.17	0.99	3.29	0.34	18.91	0.99	3.28	0.37	19.78	0.99
Suzhou(b)	4.21	0.12	5.00	1.00	4.26	0.13	5.54	1.00	4.48	0.13	6.70	1.00	4.12	0.17	8.14	1.00	4.08	0.19	8.52	1.00
Tianjin	5.40	0.25	18.99	0.99	5.02	0.29	21.06	0.99	5.13	0.34	23.36	0.99	5.25	0.41	24.61	0.99	5.34	0.44	25.04	0.99
Wuxi	3.87	0.12	11.01	0.99	3.60	0.18	13.47	0.99	3.44	0.23	16.56	0.99	3.33	0.28	17.94	0.99	3.29	0.29	18.92	0.99
Xi'an	4.13	0.12	14.71	0.99	3.89	0.14	18.49	0.99	4.06	0.15	22.21	0.99	4.55	0.20	25.39	0.99	4.88	0.23	26.69	0.99
Xinxiang	6.00	0.20	8.02	1.00	5.34	0.23	8.67	1.00	4.59	0.26	9.58	1.00	4.22	0.29	10.28	0.99	3.82	0.31	10.93	0.99
Xuchang	5.37	0.15	6.23	1.00	4.78	0.16	6.85	0.99	3.96	0.16	8.00	0.99	3.62	0.17	9.40	0.99	3.70	0.18	10.17	0.99
Xuzhou	3.17	0.23	10.24	0.99	3.14	0.24	11.97	0.99	2.98	0.24	15.12	0.99	2.87	0.23	17.45	0.99	2.87	0.23	18.89	0.99
Yangzhou	5.03	0.12	7.98	1.00	4.62	0.16	8.97	1.00	4.07	0.19	10.10	0.99	3.86	0.23	11.35	0.99	4.07	0.25	12.01	0.99
Zhengzhou	5.09	0.19	15.55	0.99	4.75	0.19	18.14	0.99	4.60	0.21	21.39	0.99	4.43	0.26	24.66	0.99	4.51	0.30	26.86	0.99

References

1. Tian, Y.; Sun, C.W. Comprehensive carrying capacity, economic growth and the sustainable development of urban areas: A case study of the Yangtze River Economic Belt. *J. Clean Prod.* **2018**, *195*, 486–496. [CrossRef]
2. Jing, S.Q.; Wang, J.F.; Xu, C.D.; Yang, J.T. Tree-like evolution pathways of global urban land expansion. *J. Clean Prod.* **2022**, *378*, 134562. [CrossRef]
3. Yang, J.; Huang, X. The 30 m annual land cover dataset and its dynamics in China from 1990 to 2019. *Earth Syst. Sci. Data* **2021**, *13*, 3907–3925. [CrossRef]
4. Peng, J.; Yang, Y.; Liu, Y.X.; Hu, Y.N.; Du, Y.Y.; Meersmans, J.; Qiu, S.J. Linking ecosystem services and circuit theory to identify ecological security patterns. *Sci. Total Environ.* **2018**, *644*, 781–790. [CrossRef]
5. Wu, Y.Y.; Xi, X.C.; Tang, X.; Luo, D.M.; Gu, B.J.; Lam, S.K.; Vitousek, P.M.; Chen, D.L. Policy distortions, farm size, and the overuse of agricultural chemicals in China. *Proc. Natl. Acad. Sci. USA* **2018**, *115*, 7010–7015. [CrossRef] [PubMed]
6. Beaumont, N.J.; Aanesen, M.; Austen, M.C.; Borger, T.; Clark, J.R.; Cole, M.; Hooper, T.; Lindeque, P.K.; Pasco, C.; Wyles, K.J. Global ecological, social and economic impacts of marine plastic. *Mar. Pollut. Bull.* **2019**, *142*, 189–195. [CrossRef]
7. Maji, K.J.; Ye, W.F.; Arora, M.; Nagendra, S.M.S. PM2.5-related health and economic loss assessment for 338 Chinese cities. *Environ. Int.* **2018**, *121*, 392–403. [CrossRef]
8. Zhou, Y.; Kong, Y.; Wang, H.K.; Luo, F.Y. The impact of population urbanization lag on eco-efficiency: A panel quantile approach. *J. Clean Prod.* **2020**, *244*, 118664. [CrossRef]
9. Ma, L.B.; Cheng, W.J.; Qi, J.H. Coordinated evaluation and development model of oasis urbanization from the perspective of new urbanization: A case study in Shandan County of Hexi Corridor, China. *Sustain. Cities Soc.* **2018**, *39*, 78–92. [CrossRef]
10. Jiang, S.N.; Zhang, Z.K.; Ren, H.; Wei, G.E.; Xu, M.H.; Liu, B.L. Spatiotemporal Characteristics of Urban Land Expansion and Population Growth in Africa from 2001 to 2019: Evidence from Population Density Data. *ISPRS Int. J. Geo-Inf.* **2021**, *10*, 584. [CrossRef]
11. He, C.Y.; Liu, Z.F.; Gou, S.Y.; Zhang, Q.F.; Zhang, J.S.; Xu, L.L. Detecting global urban expansion over the last three decades using a fully convolutional network. *Environ. Res. Lett.* **2019**, *14*, 16. [CrossRef]
12. United Nations Population Fund (UNFPA). Urbanization. Available online: <http://www.unfpa.org/urbanization> (accessed on 3 October 2016).
13. d’Amour, C.B.; Reitsma, F.; Baiocchi, G.; Barthel, S.; Guneralp, B.; Erb, K.H.; Haberl, H.; Creutzig, F.; Seto, K.C. Future urban land expansion and implications for global croplands. *Proc. Natl. Acad. Sci. USA* **2017**, *114*, 8939–8944. [CrossRef]
14. Schwarz, N.; Lautenbach, S.; Seppelt, R. Exploring indicators for quantifying surface urban heat islands of European cities with MODIS land surface temperatures. *Remote Sens. Environ.* **2011**, *115*, 3175–3186. [CrossRef]
15. Wei, S.Y.; Chen, Q.J.; Wu, W.B.; Ma, J. Quantifying the indirect effects of urbanization on urban vegetation carbon uptake in the megacity of Shanghai, China. *Environ. Res. Lett.* **2021**, *16*, 11. [CrossRef]
16. Liu, H.; Hao, Y.; Zhang, W.H.; Zhang, H.Y.; Gao, F.; Tong, J.P. Online urban-waterlogging monitoring based on a recurrent neural network for classification of microblogging text. *Nat. Hazards Earth Syst. Sci.* **2021**, *21*, 1179–1194. [CrossRef]
17. Liu, H.X.; Han, B.L.; Wang, L. Modeling the spatial relationship between urban ecological resources and the economy. *J. Clean Prod.* **2018**, *173*, 207–216. [CrossRef]
18. Shi, K.F.; Shen, J.W.; Wang, L.; Ma, M.G.; Cui, Y.Z. A multiscale analysis of the effect of urban expansion on PM2.5 concentrations in China: Evidence from multisource remote sensing and statistical data. *Build. Environ.* **2020**, *174*, 106778. [CrossRef]
19. Lu, Y.W.; Zhai, G.F.; Zhou, S.T.; Shi, Y.J. Risk reduction through urban spatial resilience: A theoretical framework. *Hum. Ecol. Risk Assess.* **2021**, *27*, 921–937. [CrossRef]
20. Liu, X.P.; Li, X.; Chen, Y.M.; Tan, Z.Z.; Li, S.Y.; Ai, B. A new landscape index for quantifying urban expansion using multi-temporal remotely sensed data. *Lands. Ecol.* **2010**, *25*, 671–682. [CrossRef]
21. Liu, J.; Xu, Q.L.; Yi, J.H.; Huang, X. Analysis of the heterogeneity of urban expansion landscape patterns and driving factors based on a combined Multi-Order Adjacency Index and Geodetector model. *Ecol. Indic.* **2022**, *136*, 108655. [CrossRef]
22. Jiao, L.M. Urban land density function: A new method to characterize urban expansion. *Lands. Urban Plan.* **2015**, *139*, 26–39. [CrossRef]
23. Wang, J.F.; Li, X.H.; Christakos, G.; Liao, Y.L.; Zhang, T.; Gu, X.; Zheng, X.Y. Geographical Detectors-Based Health Risk Assessment and its Application in the Neural Tube Defects Study of the Heshun Region, China. *Int. J. Geogr. Inf. Sci.* **2010**, *24*, 107–127. [CrossRef]
24. Liu, Y.; Hu, W.; Wang, S.W.; Sun, L.Y. Eco-environmental effects of urban expansion in Xinjiang and the corresponding mechanisms. *Eur. J. Remote Sens.* **2021**, *54*, 132–144. [CrossRef]
25. Zhou, X.Z.; Wen, H.J.; Zhang, Y.L.; Xu, J.H.; Zhang, W.G. Landslide susceptibility mapping using hybrid random forest with GeoDetector and RFE for factor optimization. *Geosci. Front.* **2021**, *12*, 101211. [CrossRef]
26. Wang, H.Y.; Qin, F.; Xu, C.D.; Li, B.; Guo, L.P.; Wang, Z. Evaluating the suitability of urban development land with a Geodetector. *Ecol. Indic.* **2021**, *123*, 107339. [CrossRef]
27. Xu, Q.R.; Zheng, X.Q.; Zhang, C.X. Quantitative Analysis of the Determinants Influencing Urban Expansion: A Case Study in Beijing, China. *Sustainability* **2018**, *10*, 1630. [CrossRef]
28. Yang, S.; Jiang, Q.; Sanchez-Barricarte, J.J. China’s fertility change: An analysis with multiple measures. *Popul. Health Metr.* **2022**, *20*, 12. [CrossRef]

29. Jiang, Q.B.; Zhang, C.L. Recent sex ratio at birth in China. *BMJ Glob. Health* **2021**, *6*, 11. [[CrossRef](#)]
30. Quanbao, J.; Shuzhuo, L.; Marcus, W.F. Demographic Consequences of Gender Discrimination in China: Simulation Analysis of Policy Options. *Popul. Res. Policy Rev.* **2011**, *30*, 619–638. [[CrossRef](#)]
31. Yang, M.Q.; Rosenberg, M.W.; Li, J. Spatial Variability of Health Inequalities of Older People in China and Related Health Factors. *Int. J. Environ. Res. Public Health* **2020**, *17*, 1739. [[CrossRef](#)]
32. Zhu, B.; Fu, Y.; Liu, J.L.; He, R.X.; Zhang, N.; Mao, Y. Detecting the priority areas for health workforce allocation with LISA functions: An empirical analysis for China. *BMC Health Serv. Res.* **2018**, *18*, 14. [[CrossRef](#)] [[PubMed](#)]
33. Zhou, J.; Walker, A. The impact of community care services on the preference for ageing in place in urban China. *Health Soc. Care Community* **2021**, *29*, 1041–1050. [[CrossRef](#)]
34. Peng, X.Z. China's Demographic History and Future Challenges. *Science* **2011**, *333*, 581–587. [[CrossRef](#)] [[PubMed](#)]
35. Li, L.S. Measurement of the Correlation Degree between Rural Family Fertility Willingness and the Development of China's Labor Original Equipment Manufacturing Industry. *Comput. Intell. Neurosci.* **2022**, *2022*, 11. [[CrossRef](#)] [[PubMed](#)]
36. Yu, X.; Wang, P. Economic effects analysis of environmental regulation policy in the process of industrial structure upgrading: Evidence from Chinese provincial panel data. *Sci. Total Environ.* **2021**, *753*, 142004. [[CrossRef](#)] [[PubMed](#)]
37. Qiu, Q.W.; Zhang, R.G. Impact of environmental effect on industrial structure of resource-based cities in western China. *Environ. Sci. Pollut. Res.* **2023**, *30*, 6401–6413. [[CrossRef](#)]
38. Zhang, H.; Li, Y.; Zhang, Q.P.; Chen, D.J. Route Selection of Multimodal Transport Based on China Railway Transportation. *J. Adv. Transp.* **2021**, *2021*, 12. [[CrossRef](#)]
39. Yin, G.J.; Peng, J.H. The Correlation between Coastal Economic Development and Inland Transportation Smoothness. *J. Coast. Res.* **2020**, *106*, 247–250. [[CrossRef](#)]
40. Wu, J.; Cui, C.Y.; Mei, X.L.; Xu, Q.S.; Zhang, P. Migration of manufacturing industries and transfer of carbon emissions embodied in trade: Empirical evidence from China and Thailand. *Environ. Sci. Pollut. Res.* **2021**, *30*, 25037–25049. [[CrossRef](#)]
41. Pretscher, A.; Kauzner, S.; Rohleder, N.; Becker, L. Associations between social burden, perceived stress, and diurnal cortisol profiles in older adults: Implications for cognitive aging. *Eur. J. Ageing* **2021**, *18*, 575–590. [[CrossRef](#)]
42. James, K.; Thompson, C.; Holder Nevins, D.; Donaldson Davis, K.; Willie-Tyndale, D.; McKoy Davis, J.; Chin-Bailey, C.; Eldemire-Shearer, D. Socio-demographic, Health and Functional Status Correlates of Caregiver Burden Among Care Recipients Age 60 Years and Older in Jamaica. *J. Community Health* **2021**, *46*, 174–181. [[CrossRef](#)] [[PubMed](#)]
43. Krings, M.F.; van Wijngaarden, J.D.H.; Yuan, S.S.; Huijsman, R. China's Elder Care Policies 1994–2020: A Narrative Document Analysis. *Int. J. Environ. Res. Public Health* **2022**, *19*, 6141. [[CrossRef](#)]
44. Dong, B.R.; Ding, Q.F. Aging in China: A Challenge or an Opportunity? *J. Am. Med. Dir. Assoc.* **2009**, *10*, 456–458. [[CrossRef](#)]
45. Li, H.B.; Li, H.T.; Guo, S.Y.; Fan, X.L.; Liu, F.Y. Study on Group Differences in Migrant Workers' Urban Integration in China. *Front. Integr. Neurosci.* **2022**, *16*, 8. [[CrossRef](#)] [[PubMed](#)]
46. Jin, X.Z.; Ren, T.Z.; Mao, N.N.; Chen, L.L. To Stay or to Leave? Migrant Workers' Decisions During Urban Village Redevelopment in Hangzhou, China. *Front. Public Health* **2021**, *9*, 11. [[CrossRef](#)] [[PubMed](#)]
47. Li, Y.J.; Kong, X.S.; Zhu, Z.Q. Multiscale analysis of the correlation patterns between the urban population and construction land in China. *Sustain. Cities Soc.* **2020**, *61*, 102326. [[CrossRef](#)]
48. Sun, F.H.; Miao, X.M.; Feng, X.Y.; Ye, C.L. Understanding the Impact of Rural Returnees' Hometown Identity on Their Successful Entrepreneurship with the Operations Research Framework. *Math. Probl. Eng.* **2022**, *2022*, 13. [[CrossRef](#)]
49. Gao, J.; O'Neill, B.C. Mapping global urban land for the 21st century with data-driven simulations and Shared Socioeconomic Pathways. *Nat. Commun.* **2020**, *11*, 12. [[CrossRef](#)]
50. Song, S.X.; He, C.Y.; Liu, Z.F.; Qi, T. Evaluating the influences of urban expansion on multiple ecosystem services in drylands. *Landsc. Ecol.* **2022**, *37*, 2783–2802. [[CrossRef](#)]
51. Chang, D.K.; Wang, Q.J.; Xie, J.J.; Yang, J.Y.; Xu, W.T. Research on the Extraction Method of Urban Built-Up Areas With an Improved Night Light Index. *IEEE Geosci. Remote Sens. Lett.* **2022**, *19*, 5. [[CrossRef](#)]
52. Li, X.C.; Gong, P.; Zhou, Y.Y.; Wang, J.; Bai, Y.Q.; Chen, B.; Hu, T.Y.; Xiao, Y.X.; Xu, B.; Yang, J.; et al. Mapping global urban boundaries from the global artificial impervious area (GAIA) data. *Environ. Res. Lett.* **2020**, *15*, 094044. [[CrossRef](#)]
53. Yang, J.; Li, J.; Xu, F.; Li, S.; Zheng, M.; Gong, J. Urban development wave: Understanding physical spatial processes of urban expansion from density gradient of new urban land. *Comput. Environ. Urban Syst.* **2022**, *97*, 101867. [[CrossRef](#)]
54. Zhang, X.; Jie, X.W.; Ning, S.N.; Wang, K.; Li, X.P. Coupling and coordinated development of urban land use economic efficiency and green manufacturing systems in the Chengdu-Chongqing Economic Circle. *Sustain. Cities Soc.* **2022**, *85*, 104012. [[CrossRef](#)]
55. Lin, X.Q.; Wang, Y. Measuring Resource, Environmental, and Economic Efficiency of China's Urban Agglomerations Based on Hybrid Directional Distance Function. *J. Urban Plan. Dev* **2019**, *145*, 10. [[CrossRef](#)]
56. Yang, C.S.; Yu, B.L.; Chen, Z.Q.; Song, W.; Zhou, Y.Y.; Li, X.; Wu, J.P. A Spatial-Socioeconomic Urban Development Status Curve from NPP-VIIRS Nighttime Light Data. *Remote Sens.* **2019**, *11*, 2398. [[CrossRef](#)]
57. Zhou, Y.; Chen, M.X.; Tang, Z.P.; Mei, Z.A. Urbanization, land use change, and carbon emissions: Quantitative assessments for city-level carbon emissions in Beijing-Tianjin-Hebei region. *Sustain. Cities Soc.* **2021**, *66*, 102701. [[CrossRef](#)]
58. Tang, M.G.; Li, Z.; Hu, F.X.; Wu, B.J. How does land urbanization promote urban eco-efficiency? The mediating effect of industrial structure advancement. *J. Clean Prod.* **2020**, *272*, 122798. [[CrossRef](#)]

59. Yu, S.S.; Zhang, Z.X.; Liu, F.; Wang, X.; Hu, S.G. Assessing Interannual Urbanization of China's Six Megacities Since 2000. *Remote Sens.* **2019**, *11*, 2138. [[CrossRef](#)]
60. Ye, C.H.; Sun, C.W.; Chen, L.T. New evidence for the impact of financial agglomeration on urbanization from a spatial econometrics analysis. *J. Clean Prod.* **2018**, *200*, 65–73. [[CrossRef](#)]
61. Jiang, J.K.; Zhu, S.L.; Wang, W.H. Carbon Emissions, Economic Growth, Urbanization, and Foreign Trade in China: Empirical Evidence from ARDL Models. *Sustainability* **2022**, *14*, 9396. [[CrossRef](#)]
62. Zhao, R.; Jiao, L.; Xu, G.; Xu, Z.; Dong, T. The relationship between urban spatial growth and population density change. *Acta Geogr. Sin.* **2020**, *75*, 695–707.
63. Zhao, J.Q.; Xiao, Y.; Sun, S.Q.; Sang, W.G.; Axmacher, J.C. Does China's increasing coupling of 'urban population' and 'urban area' growth indicators reflect a growing social and economic sustainability? *J. Environ. Manag.* **2022**, *301*, 113932. [[CrossRef](#)]
64. Liu, S.S.; Liao, Q.P.; Liang, Y.; Li, Z.F.; Huang, C.B. Spatio-Temporal Heterogeneity of Urban Expansion and Population Growth in China. *Int. J. Environ. Res. Public Health* **2021**, *18*, 3031. [[CrossRef](#)] [[PubMed](#)]
65. Lin, X.Y.; Wang, P. Relationship between Rising Housing Prices and Reduction in Urban Agglomeration. *J. Urban Plan. Dev* **2020**, *146*, 13. [[CrossRef](#)]
66. Huang, Q.Y.; Liu, Y.H. The Coupling between Urban Expansion and Population Growth: An Analysis of Urban Agglomerations in China (2005–2020). *Sustainability* **2021**, *13*, 7250. [[CrossRef](#)]
67. Alvarez-Berrios, N.L.; Pares-Ramos, I.K.; Aide, T.M. Contrasting Patterns of Urban Expansion in Colombia, Ecuador, Peru, and Bolivia Between 1992 and 2009. *Ambio* **2013**, *42*, 29–40. [[CrossRef](#)]
68. Xu, S.C.; Miao, Y.M.; Gao, C.; Long, R.Y.; Chen, H.; Zhao, B.; Wang, S.X. Regional differences in impacts of economic growth and urbanization on air pollutants in China based on provincial panel estimation. *J. Clean Prod.* **2019**, *208*, 340–352. [[CrossRef](#)]
69. Yang, J.; Zhang, W.; Zhang, Z.Y. Impacts of urbanization on renewable energy consumption in China. *J. Clean Prod.* **2016**, *114*, 443–451. [[CrossRef](#)]
70. Han, J.W.; Miao, J.J.; Shi, Y.; Miao, Z. Can the semi-urbanization of population promote or inhibit the improvement of energy efficiency in China? *Sustain. Prod. Consump.* **2021**, *26*, 921–932. [[CrossRef](#)]
71. Zhang, J.X.; Deng, X.Y. Real Estate Tax, Housing Price, and Housing Wealth Effect: An Empirical Research on China Housing Market. *Discrete Dyn. Nat. Soc.* **2022**, *2022*, 4809499. [[CrossRef](#)]
72. Zhai, D.; Shang, Y.S.; Wen, H.Z.; Ye, J.B. Housing Price, Housing Rent, and Rent-Price Ratio: Evidence from 30 Cities in China. *J. Urban Plan. Dev* **2018**, *144*, 04017026. [[CrossRef](#)]
73. Mostafa, A.; Wong, F.K.W.; Hui, C.M.E. Relationship between housing affordability and economic development in mainland China—Case of Shanghai. *J. Urban Plan. Dev* **2006**, *132*, 62–70. [[CrossRef](#)]

Disclaimer/Publisher's Note: The statements, opinions and data contained in all publications are solely those of the individual author(s) and contributor(s) and not of MDPI and/or the editor(s). MDPI and/or the editor(s) disclaim responsibility for any injury to people or property resulting from any ideas, methods, instructions or products referred to in the content.